less important. Indeed, several stable dialkyl complexes are known. Our results clearly show that C–H activation is kinetically favoured over C–C activation, in agreement with theoretical calculations[20,21]. This kinetic barrier for C–C cleavage is overcome here by relatively mild heating. As **3** does not react with methane, the overall C–C activation process is irreversible and is thermodynamically more favourable than the overall C–H activation sequence, although both processes are clearly possible. We cannot rigorously compare the single insertion steps at this stage. It may seem that insertion into $ArCH_2$–H and generation of Rh–H would be thermodynamically more favourable than insertion into Ar–CH_3 (bond dissociation energies (BDE) of $C_6H_5CH_2$–H and $C_6H_5CH_3$ are 88.0 ± 1 and 101.8 ± 2 kcal mol^{-1} respectively[22]). We have to remember, however, that Ar–Rh is considerably stronger than alkyl–Rh[23,24], a relationship that is particularly applicable for **2** (see X-ray structure), and that the Rh–H bond in **5** is relatively weak (spontaneous H_2 elimination from **5** indicates a BDE of Rh–H < 52 kcal mol^{-1}). Thus, metal insertion into C–C may actually prevail even in this case, even though the C–C bond is probably stronger than the C–H bond. Note that bond dissociation energies of C–H bonds do not correlate well with their relative reactivities in C–H oxidative addition[2]. Also, an sp^3–sp^2 C–C bond may be more reactive than an sp^3–sp^3 C–C bond, in line with the typically higher oxidative addition reactivity of aryl–H relative to alkyl–H.

It should be possible to find other systems in which 'precoordination' in the substrate enhances metal insertion into a C–C bond. Moreover, although C–C activation is helped here by metal precoordination, we believe that it need not be a prerequisite. This work provides hope that homogeneous activation and thus selective transformation of C–C bonds by metal insertion may be achieved quite generally. □

Received 12 May; accepted 7 July 1993.

1. Sinflet, J. H. in *Catalysis: Science and Technology* Vol. 1 (eds Anderson, J. R. & Boudart, M.) 257–300 (Springer, New York, 1981).
2. Crabtree, R. H. *Chem. Rev.* **85,** 245–269 (1985).
3. Bergman, R. G. *Science* **223,** 902–908 (1984).
4. Shilov, A. E. *Activation of Saturated Hydrocarbons by Transition Metal Complexes* (Reidal, Boston, 1984).
5. Maugh, T. H. *Science* **220,** 1262–1263 (1983).
6. Periana, R. A. & Bergman, R. G. *J. Am. chem. Soc.* **108,** 7346–7355 (1986).
7. Crabtree, R. H., Dion, R. P., Gibboni, D. J., McGrath, D. V. & Holt, E. M. *J. Am. chem. Soc.* **108,** 7222–7227 (1986).
8. Kang, J. W., Moseley, R. & Maitlis, D. M. *J. Am. chem. Soc.* **91,** 5970–5977 (1969).
9. Benfield, F. W. C. & Green, M. L. H. *J. chem. Soc. Dalton Trans.* 1324–1331 (1974).
10. Eilbracht, P. *Chem. Ber.* **113,** 542–554 (1980).
11. Suggs, J. W. & Jun, C.-H. *J. Am. chem. Soc.* **106,** 3054–3056 (1984).
12. Hartwig, J. F., Anderson, R. A. & Bergman, R. G. *J. Am. chem. Soc.* **111,** 2717–2719 (1989).
13. Watson, P. L. & Roe, D. C. *J. Am. chem. Soc.* **104,** 6471–6473 (1982).
14. Bunel, E., Burger, B. J. & Bercaw, J. E. *J. Am. chem. Soc.* **110,** 976–978 (1988).
15. Moulton, C. J. & Shaw, B. L. *J. chem. Soc. Dalton Trans.* 1020–1024 (1976).
16. Rimml, H. & Venanzi, L. M. *J. Organomet. Chem.* **259,** C6–C7 (1983).
17. Nemeh, S., Jensen, C., Binamira-Soriaga, E. & Kaska, W. C. *Organometallics* **2,** 1442–1447 (1983).
18. Milstein, D. *Accts. chem. Res.* **17,** 221–226 (1984).
19. Grove, D. M. *et al. J. Am. chem. Soc.* **104,** 6609–6616 (1982).
20. Blomberg, M. R. A., Siegbahn, P. E. M., Nagashima, U. & Wennerberg, *J. J. Am. chem. Soc.* **113,** 424–433 (1991).
21. Low, J. J. & Goddard, W. A. *Organometallics* **5,** 609–622 (1986).
22. McMillen, D. F. & Golden, D. M. *A. Rev. Phys. Chem.* **33,** 493–532 (1982).
23. Jones, W. D. & Feher, F. J. *J. Am. chem. Soc.* **106,** 1650–1663 (1984).
24. Martinho-Simoes, J. A. & Beauchamp, J. L. *Chem. Rev.* **90,** 629–688 (1990).

ACKNOWLEDGEMENTS. We thank S. Cohen for the X-ray structural analysis and M. Portnoy for discussions. The possible involvement of intermediate **10** in the reaction scheme in Fig. 4 was suggested by an anonymous referee. This work was supported by the Israel Science Foundation, administered by the Israel Academy of Sciences and Humanities.

Evidence for slow mixing across the pycnocline from an open-ocean tracer-release experiment

James R. Ledwell*, Andrew J. Watson† & Clifford S. Law†

* Applied Ocean Physics and Engineering, Woods Hole Oceanographic Institution, Woods Hole, Massachusetts 02543, USA
† Plymouth Marine Laboratory, Prospect Place, West Hoe, Plymouth PL1 3DH, UK

THE distributions of heat, salt and trace substances in the ocean thermocline depend on mixing along and across surfaces of equal density (isopycnal and diapycnal mixing, respectively). Measurements of the invasion of anthropogenic tracers, such as bomb tritium and ^{3}He (see, for example, refs 1 and 2), have indicated that isopycnal processes dominate diapycnal mixing, and turbulence measurements have suggested that diapycnal mixing is small[3,4], but it has not been possible to measure accurately the diapycnal diffusivity. Here we report such a measurement, obtained from the vertical dispersal of a patch of the inert compound SF_6 released in the open ocean. The diapycnal diffusivity, averaged over hundreds of kilometres and five months, was 0.11 ± 0.02 cm^2 s^{-1}, confirming previous estimates[1–4]. Such a low diffusivity can support only a rather small diapycnal flux of nitrate into the euphotic zone; it justifies the neglect of diapycnal mixing in dynamic models of the thermocline[25–27], and implies that heat, salt and tracers must penetrate the thermocline mostly by transport along, rather than across, density surfaces.

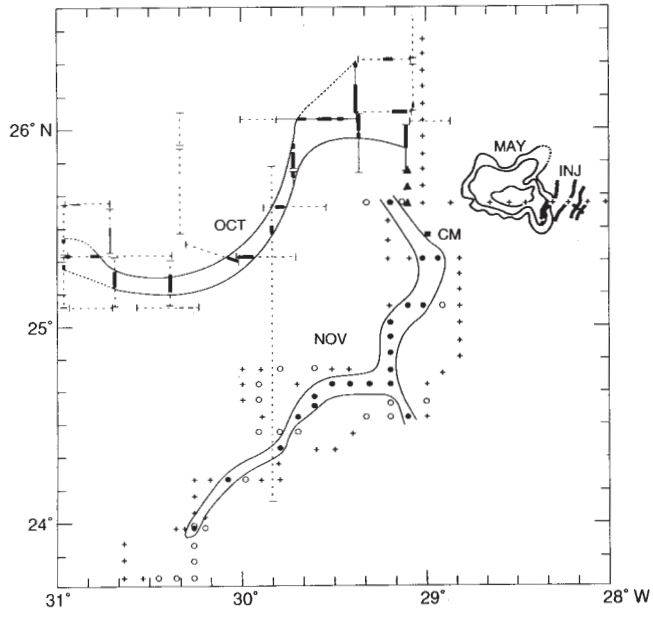

FIG. 1 Evolution of the lateral distribution of the tracer. The injection streaks are shown as short heavy lines near 26° N, 28° W. The contours just to the west show the patch later in May 1992. Heavy lines (further to the west) show tracks for the October survey, where the concentration C at the target surface was >500 fM; light solid lines, C was between 100 and 500 fM; dashed lines, $C \sim 0$. Solid triangles indicate bottle stations occupied at the end of the October cruise, with $C > 300$ fM. Station symbols for the November survey are: plus signs, $C < 30$ fM; open circles, $C = 30$–300 fM; filled circles, $C > 300$ fM. A fine curve has been drawn to envelop the high C regions for the two surveys. CM marks the location of the central mooring for the Subduction experiment.

Our experiment, which is a component of the World Ocean Circulation Experiment (WOCE), began with the release of 139 kg (950 mol) of sulphur hexafluoride (SF_6) on a target density surface about 310 m deep, at a location 1,200 km west of the Canary Islands. SF_6 is an inert and non-toxic compound[5] which has proven to be conservative in pilot experiments[6,7]. Yet it is detectable in amounts of less than 10^{-16} moles with a shipboard gas chromatograph equipped with an electron capture detector[8]. It is this sensitivity, and the oceanic background of less than 1 fM (10^{-15} M)[9], which makes the large scale of the experiment possible.

The tracer was released from R/V *Oceanus* in a series of streaks between 5 and 13 May 1992 (INJ in Fig. 1). The injection package consisted of a pumping system that atomizes liquid SF_6 through a 50-micron sapphire orifice for efficient dissolution. It was towed at 0.5 m s^{-1} while being held automatically within a few metres of the target density surface.

Sampling of the tracer commenced from RRS *Charles Darwin*, 14–31 May 1992, by towing a vertical array of 19 samplers, spaced 2 to 6 m apart, through the patch at 0.5 m s^{-1}. Each sampler took in water over a period of ~4 h, the array yielding a vertical profile averaged over the track. An 18-chamber sampler was located at the centre of the array, each chamber integrating over ~350 m of the track. Virtually all of the tracer was found in a patch just west of the injection (MAY in Fig. 1), with the help of acoustically tracked floats released with the tracer[10]. The patch seemed to be made up of streaks of ~1,500 m width, with spacing between streak centres being of the order of 3,000 m; that is, the original injection streaks seemed well on their way towards filling in the patch area.

For the second survey, 26 September to 18 October from *Oceanus*, 23 samplers were spaced 4–6 m apart on the wire, the tow speed and duration were increased to 1.2 m s^{-1} and 7 h, respectively, and the central sampler had 50 chambers, each integrating laterally over 600 m. Ranges to the tracking floats were supplemented with previous estimates of the mean drift in the region[11,12], and with the drift of another nearby float provided by R. Davis. All of these sources indicated a mean drift of about 1 cm s^{-1} to the west or southwest, guiding the choice of starting point for the October survey near 24° 07′ N, 29° 50′ W (Fig. 1).

The initial search encountered just one intense streak, about 8 km wide, at 25° 29′ N, 29° 50′ W. This streak was found to stretch at least 200 km, the west end branching into a number of thin, weak streaks, and the northeast end branching into a number of wider, stronger limbs covering a region about 50 km across. Concentrations were of the order of 1,000 fM within the streak, and usually fell abruptly through 100 fM at the edges of the streak. Fifteen to twenty per cent of the tracer was found on this cruise.

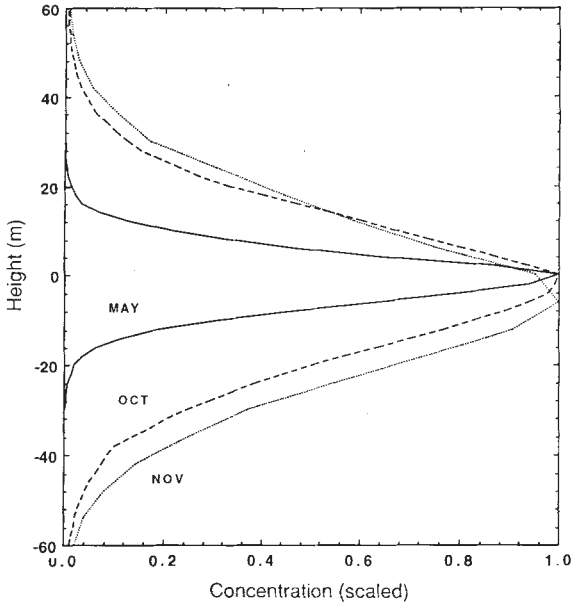

FIG. 2 Evolution of the vertical distribution of the tracer. The mean profiles have been scaled so that the widths can be compared.

It was found during the October cruise that the diapycnal distribution of the tracer could be sampled with conventional bottle casts made every 9 km. This finding implies a surprising amount of cross-streak homogeneity, and also that future surveys can cover an area more quickly. Indeed, bottle casts were used to continue the tracer survey from *Oceanus* in November, together with turbulence studies[13,14]. The tracer was relocated near the east end of the streak found in October, and followed for 250 km to the southwest (NOV in Fig. 1). We estimate that 10–15% more of the tracer was found on this cruise, unless we resampled some of the same tracer encountered in October, which seems unlikely. If all of the tracer were distributed in a manner similar to that shown in Fig. 1, the total unfolded streak length would be ~1,800 km.

Figure 1 shows a clear separation between the mesoscale, represented by the radii of curvature of different parts of the streak, of the order of 100 km, and the finescale, represented by the r.m.s. cross-streak width, of the order of 3 km. According to a scale analysis[15] and a numerical model[16], this r.m.s. width implies an efficient process of dispersion at scales of 1 to 10 km. The unfolded length L of a tracer streak is thought to grow exponentially with time as the area occupied by the streak grows from the finescale to the mesoscale: $L = L_0 e^{\gamma t}$, where γ is of the order of the r.m.s. mesoscale strain rate. The value of γ corresponding to $L_0 = 40$ km from the first survey, and the $L = 1{,}800$ km estimated for the fall, is 3×10^{-7} s^{-1}. The r.m.s. width σ_y of the streak is set in the models by a balance between lateral convergence associated with the strain and lateral eddy diffusion: $\sigma_y^2 = K_y/\gamma$, which gives an effective lateral eddy diffusivity K_y of the order of 3 m^2 s^{-1}.

The streak width is not necessarily in steady state, and other processes such as cross-streak shear in the along-streak direction could be elongating the streak, as has been pointed out by E. Kunze (personal communication). But any scheme requires K_y to be of the order of 1 m^2 s^{-1} to give the 40-fold increase in the area actually stained by the tracer and the concomitant decrease in maximum concentration over the 5-month period.

This value of K_y is at least an order of magnitude larger than the small scale lateral eddy diffusivity expected from the interaction between vertical shear of the internal waves and vertical mixing[17]. Weaker but more persistent vertical shears, associated with the mesoscale eddy field or small scale vortices[18], could be responsible for the observed lateral dispersion, however[17].

Each survey shown in Fig. 1 produced 20 to 30 vertical tracer profiles, which were averaged as a function of height h above the target density surface (Fig. 2). An estimate of the diapycnal eddy diffusivity K_z can be obtained from the increase of the second moment M_2 of these mean profiles with time t according to: $2K_z = dM_2/dt$.

Values for M_2, estimated as the second moment of gaussian functions fitted to the mean profiles, are shown in Fig. 3 for two cases. The upper point for each survey is M_2 calculated relative to the target density surface; the lower point is M_2 relative to the centre of mass, which is shifted downwards by 0.8 m, 2.7 m and 5.1 m for the May, October and November surveys, respectively. Use of the lower points would be appropriate if these shifts were artefacts, whereas the upper ones would be appropriate if the shifts are the result of an oceanographic phenomenon, such as shear distortion. The difference in the value of K_z inferred from the best-fit slope for the two cases is only 7%. The middle ground results in an estimate of $K_z = 0.11 \pm 0.02$ cm^2 s^{-1}. This result agrees with preliminary estimates of the eddy diffusivity of density and temperature from measurements of turbulent dissipation rates during a broad site survey in April 1992 (ref. 19).

There are adjustments to be made to this estimate of K_z owing

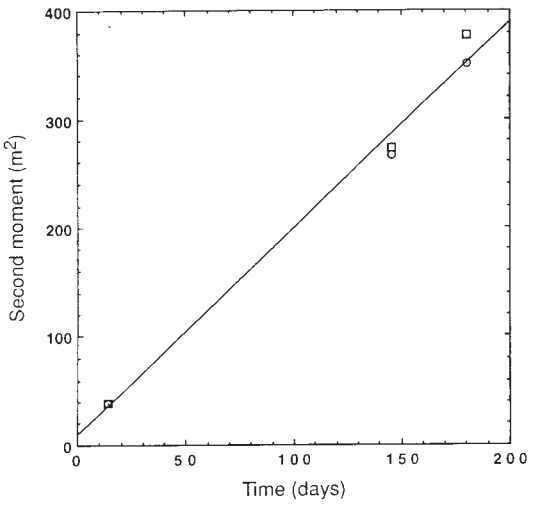

FIG. 3 Growth of the second moment of the vertical tracer distribution. Squares are for raw M_2, circles are for the centre of mass shifted to $h=0$. The line is for $K_z=0.11$ cm^2 s^{-1}.

to the variation of density at fixed h, and to changes in mean stratification between May and November. Preliminary estimates indicate that these adjustments nearly cancel one another and contribute most of the uncertainty in K_z.

This estimate of K_z applies to the part of the ocean sampled by the tracer we found, namely a volume of space–time of the order of 10^{17} m^3 s. One cannot prove that the unsampled part of the patch has the same vertical distribution. But the evidence from the site survey is that the turbulent dissipation rates were uniform over the region[19]. Measures of temporal variability in the dynamics driving the mixing will be available from current metres on the central mooring[20] of the Subduction Experiment, another component of WOCE, (Fig. 1), and from a specially designed float[21].

These data promise extrapolation of our measurement of K_z to a large fraction of the upper 1,000 m of the global ocean in stratified waters below the region mixed by cooling each winter. This stratified layer is important as a reservoir of nutrients for the euphotic zone, and as a capacitor for perturbations of atmospheric temperature and carbon dioxide associated with climate change.

If a value for K_z of 0.11 cm^2 s^{-1} were to prove typical of the upper ocean, then diapycnal mixing would not be the dominant transport mechanism within this layer for many processes. For example, the flux of nitrate through the upper layer to support 'new' biological productivity in the euphotic zone would be of the order of 0.01 M m^{-2} yr^{-1}. Although this flux is about 50% of that required by estimates of productivity for the subtropical oceans based on incubations[22], it is only 2% of the flux required by *in situ* oxygen and ^{3}He budgets[23]. Thus, other nitrate transport mechanisms may be operating (see, for example ref. 24).

Also, if K_z is so small, the dynamics of the upper ocean can be modelled by neglecting diapycnal processes in the stratified interior, as it often has been[25–27]. Furthermore, the response of this layer to a perturbation of atmospheric temperature or carbon dioxide would not be governed by diapycnal mixing in the interior. Rather, transport of nitrate, heat, salt and trace constituents would be dominated by advection along density surfaces, coupled with mixing at the surface and other boundaries.

A final sampling of the tracer patch in the spring of 1993 will provide a measurement of K_z for a winter period, and further information about lateral processes. Future experiments, especially in the deeper ocean and near boundaries, could clarify where mixing is occurring and its strength.

Note added in proof: Virtually all the tracer was found in the spring, in a 600,000-km^2 patch rich with streaks. Preliminary estimates are that K_z for the entire year was 0.15 cm^2 s^{-1}, suggesting somewhat more vigorous mixing in the winter. □

Received 10 February; accepted 25 June 1993.

1. Rooth, C. G. & Ostlund, H. G. *Deep-Sea Res.* **19,** 481–492 (1972).
2. Jenkins, W. J. *J. Mar. Res.* **38,** 533–569 (1980).
3. Moum, J. N. & Osborn, T. R. *J. phys. Oceanogr.* **16,** 1250–1259 (1986).
4. Gregg, M. C. J. *geophys. Res.* **94,** 9686–9698 (1989).
5. Lester, D. & Greenberg, L. A. *Arch. Ind. Hyg. Occup. Med.* **2,** 348–349 (1950).
6. Ledwell, J. R. & Watson, A. J. *J. geophys. Res.* **96,** 8695–8718 (1991).
7. Watson, A. J., Ledwell, J. R. & Sutherland, S. C. *J. geophys. Res.* **96,** 8719–8725 (1991).
8. Wanninkhof, R., Ledwell, J. R. & Watson, A. J. *J. geophys. Res.* **96,** 8733–8740 (1991).
9. Watson, A. J. & Liddicoat, M. I. *Atmos. Environ.* **19,** 1477–1484 (1985).
10. Price, J., McKee, T., Valdes, J., Richardson, P. & Armi, L. Report. 86–31, Woods Hole Oceanographic Institution (Woods Hole, MA, 1986).
11. Armi, L. & Stommel, H. *J. phys. Oceanogr.* **13,** 828–857 (1983).
12. Thiele, G. *et al. J. phys. Oceanogr.* **16,** 814–826 (1986).
13. Oakey, N. S. *IEEE J. Ocean. Engng* **13,** 124–128 (1988).
14. Duda, T. F., Cox, C. S. & Deaton, T. K. *J. Atmos. Ocean Tech.* **5,** 16–33 (1988).
15. Garrett, C. *Dyn. Atmos. Oceans* **7,** 265–277 (1983).
16. Haidvogel, D. B. & Keffer, T. *Dynam. Atmos. Oceans* **8,** 1–40 (1984).
17. Young, W. R., Rhines, P. B. & Garrett, C. J. R. *J. phys. Oceanogr.* **12,** 515–527 (1982).
18. Muller, P., Lien, R.-C. & Williams, R. *J. phys. Oceanogr.* **18,** 401–416 (1988).
19. Montgomery, E., Schmitt, R. W., Toole, J. M. & Polzin, K. L. *EOS* **73,** 321 (1992).
20. Hosom, D. S., Weller, R. A., Prada, K. E. & Trask, R. P. *Proc. Mar. Tech. Soc.* **1,** 206–210 (1991).
21. Williams, A. J., Converse, C. H. & Nicholson, J. *Am. Soc. mech. Engng, OED* **12,** 25–29 (1987).
22. Eppley, R. W. & Peterson, B. J. *Nature* **282,** 677–680 (1979).
23. Jenkins, W. J. *Nature* **331,** 521–523 (1988).
24. Vilareal, T. A., Altabet, M. A. & Culver-Rymsza, K. *Nature* **363,** 709–712 (1993).
25. Welander, P. *Tellus* **11,** 309–318 (1959).
26. Luyten, J. R., Pedlosky, J. & Stommel, H. *J. phys. Oceanogr.* **13,** 292–309 (1983).
27. Huang, R. X. *Rev. Geophys. suppl.* 590–609 (1991).

ACKNOWLEDGEMENTS. The tracer experiment is an outgrowth of suggestions by W. S. Broecker, J. Shepherd and J. Lovelock. We thank S. Becker, D. Ciochetto, E. Clark, K. Doherty, T. Donoghue, K. Fairhurst, C. Fernandez, B. Guest, S. Kery, M. Klas, C. Kinkade, M. Liddicoat, K. Lubcke, C. Marquette, A. Martin, P. Nightingale, N. Oakey, R. Oxburgh, H. Rochat, B. Ruddick, S. Sutherland, K. Tedesco, J. White, RVS in the UK, the crews of *Darwin* and *Oceanus*, our home laboratories for their help, and E. Kunze for comments on the manuscript. The experiment has been supported by the US NSF and the UK Natural Environment Research Council.

A δ^{13}C record of late Quaternary climate change from tropical peats in southern India

R. Sukumar*, R. Ramesh†, R. K. Pant† & G. Rajagopalan‡

* Centre for Ecological Sciences, Indian Institute of Science, Bangalore–560 012, India
† Physical Research Laboratory, Ahmedabad–380 009, India
‡ Birbal Sahni Institute of Palaeobotany, Lucknow–226 007, India

STABLE-ISOTOPE ratios of carbon in soils or lake sediments[1–3] and of oxygen and hydrogen in peats[4,5] have been found to reflect past moisture variations and hence to provide valuable palaeoclimate records. Previous applications of the technique to peat have been restricted to temperate regions, largely because tropical climate variations are less pronounced, making them harder to resolve. Here we present a δ^{13}C record spanning the past 20 kyr from peats in the Nilgiri hills, southern India. Because the site is at high altitude (>2,000 m above sea level), it is possible to resolve a clear climate signal. We observe the key climate shifts that are already known to have occurred during the last glacial maximum (18 kyr ago) and the subsequent deglaciation. In addition, we observe an arid phase from 6 to 3.5 kyr ago, and a short, wet phase about 600 years ago. The latter appears to correspond to the Mediaeval Warm Period, which previously was believed to be confined to Europe and North America[6,7]. Our results therefore suggest that this event may have extended over the entire Northern Hemisphere.

The use of stable carbon isotope ratios as palaeoclimatic indicators is based on the different ecological requirements of the C3 and C4 plant types that have widely differing ^{13}C/^{12}C ratios.